Monolithic 3-Terminal Perovskite/Silicon HBT-Based Tandem Compatible with Industrial Silicon Bottom Cells: A Theoretical Study

MONOLITHIC 3-TERMINAL PEROVSKITE/SILICON HBT-BASED TANDEM COMPATIBLE WITH INDUSTRIAL SILICON BOTTOM CELLS: A THEORETICAL STUDY

Gemma Giliberti, Matteo Cagnoni and Federica Cappelluti
Department of Electronics and Telecommunications, Politecnico di Torino
Corso Duca degli Abruzzi 24, 10129 Torino, Italy
E-mail: gemma.giliberti@polito.it, matteo.cagnoni@polito.it, federica.cappelluti@polito.it

ABSTRACT: Perovskite/silicon tandem solar cells are among the most promising solutions to overcome the efficiency bottleneck of single-gap Si cells. Multi-terminal configurations are interesting alternatives to the more studied series connected two-terminal tandem, because they allow for looser band gap requirements and higher energy yield in the field. Among three-terminal architectures, the heterostructure bipolar transistor (HBT) solar cell offers a promising approach for the integration of the top perovskite cell with both-side contacted silicon cells, which are the industry standard. Material engineering makes it possible to prevent minority carriers transport across the interface layers between the two sub-cells, allowing them to work independently. However, the introduction of the middle contact at the interface layers requires the adoption of interdigitated contact grids for current collection, whose associated optical and resistive losses need to be minimized to not jeopardize the high efficiency potential of the intrinsic device. In this work, we use physics-based and circuit-level simulations to address such issues in the perspective of developing high efficiency large-area perovskite/silicon tandems with 3T-HBT structure.

Keywords: perovskite/silicon tandems, 3-terminal tandems, heterostructure bipolar transistor, current collecting grid photovoltaics

1 INTRODUCTION

Perovskite/silicon solar cells combine high energy efficiency and low cost and are expected to enter the market soon [1], provided that their long-term stability issues can be significantly mitigated. Research has been mostly focused on 2-terminal (2T) devices, but multi-terminal 3T and 4T configurations are drawing increasing attention because of their higher flexibility in terms of perovskite band gap. Indeed, this provides higher degrees of freedom to solve stability issues [2], and less sensitivity to spectral and temperature fluctuations, and therefore higher predicted energy yield in the field [3], [4].

3T tandems reported so far are mainly based on the idea of using an interdigitated back contact (IBC) silicon bottom cell [5][6]. However, solutions compatible with both-side contacted silicon cells, such as Al-BSF, PERX, and heterojunction [7, 8] would be of great interest, because these are the preferred choice in industry [9, 10] because of their lower complexity. Possible 3T tandem approaches could be pursued either by introducing an intermediate transparent conductive layer between the two sub-cells, as done in [11], or by adopting the heterostructure bipolar transistor (HBT) architecture [12]. The HBT architecture enables the seamless connection of two sub-cells of opposite electrical polarity, by exploiting three semiconductor regions with alternating doping and each having its own electrical contact. Since the seminal work in [12], significant progress has been reported on III-V HBT solar cells [13], that proves the feasibility of this idea. In the context of perovskite/silicon (PVK/Si) technology, we have proposed a few designs of 3T-HBT with planar [14] and textured [15] Si bottom cells, predicting high theoretical efficiency on the basis of optical and transport simulations.

However, the HBT structure requires the introduction of a middle contact at the interface layers between the two sub-cells, and the adoption of interdigitated grids for current collection. These cause optical and resistive losses that need to be carefully assessed, especially in view of the rather limited (when compared to crystalline semiconductors) electrical conductivity of the materials commonly exploited as interfacial layers, such as organic electron and hole transport layers of the perovskite cell and hydrogenated amorphous silicon of heterojunction silicon cells.

In this work, we lay the groundwork for this, by studying HBT architectures with interdigitated contact layouts by means of a mixed-mode approach that combines transport and optical simulations for characterizing the intrinsic behavior of the HBT multilayer stack with circuit-level simulations for the analysis of shading and resistive loss associated to the metal grids. We study tandem architectures based on homo- and hetero-junction silicon cells to analyze to what extent the middle contact could induce resistive mediated cross-talk between the junctions and discuss prospects for the scalability of these devices to large areas.

2 DEVICE AND MODELING

Here, we consider a *p-n-p* HBT tandem made on a c-Si homojunction cell whose structure is depicted in Fig. 1(a). To realize the three-terminal connection, we introduce top interdigitated contact (TIC) grids for the emitter and base terminals, as shown in Fig. 1(b).

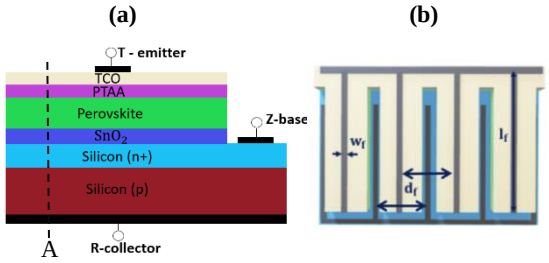

Figure 1: Example of structure of *p-n-p* 3T-HBT tandem based on *n-i-p* PVK cell combined with homojunction *n-p* Si bottom cell (a), TIC metal layout (b).

We start by analyzing the "intrinsic" device, i.e. the multilayer stack identified by cutline A in Fig. 1(a). The tandem structure is the following: from the top, thin conductive oxide (TCO) (34 nm), PTAA (11 nm) as hole transport layer (HTL), PVK (480 nm, Eg=1.55eV), SnO_2 (25 nm) electron transport layer (ETL), *n*-Si (150 nm), and 150 µm thick *p*-type c-Si. The cell architecture is completed by a 92 nm thick MgF antireflection coating. The alternate doping layers of the PVK and Si sub-cells form a structure analogous to that one of a bipolar transistor (*p*-Emitter, *n*-Base, *p*-Collector).

We use quasi-1D physics-based simulations (Transfer Matrix Method for the optical model coupled with Poisson-Drift-Diffusion for the transport model) to characterize the photovoltaic behavior of the intrinsic device.

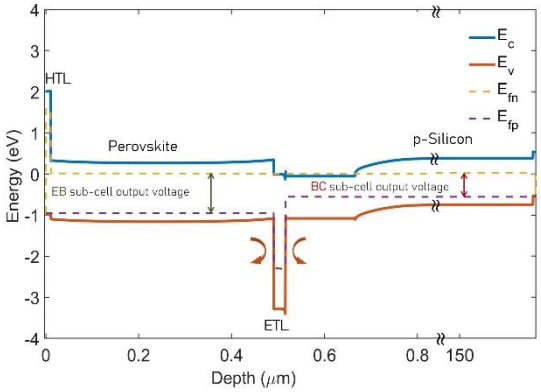

Figure 2: Energy band diagram of the *p-n-p* 3T-HBT with each junction biased at maximum power point. The dashed yellow and pink lines are the electron and hole quasi-Fermi levels, respectively.

Fig. 2 reports the device energy band diagram at maximum power point (MPP). One can see that the energy band alignment at the E/B (i.e. PVK/ETL) and B/C (i.e. n^+-Si/*p*-Si) heterointerfaces allows collection of electrons at the base contacts, whereas *repels* holes photogenerated in each sub-cell towards their respective contacts, i.e. emitter and collector, avoiding any injection from one junction to the other. This enables the perovskite and silicon layers to support a different splitting of electron and hole quasi-Fermi-levels, coherently with their own bandgap. The PVK and Si sub-cells reach open circuit voltage of 1.06 and 0.64, respectively. Owing to the independent operation of the two sub-cells, the tandem MPP takes place when each sub-cell is biased at MPP, with an overall efficiency higher than 29 % under AM1.5G.

Although the *intrinsic* performance of the HBT device is suitable for high power conversion efficiency, considering a realistic device layout as that one depicted in Fig. 1, two main effects must be carefully analyzed:

(i) the possible sub-cells cross-talk due to the parasitic resistance induced by the lateral transport across the thin base region (Fig. 1(b));

(ii) the implications of optical and resistive losses caused by the additional contact grid in terms of scalability to large areas.

To assess these effects, we resort to circuit-level simulations with the equivalent circuit model in Fig. 3. We extract the compact model of the intrinsic device by fitting the photovoltaic characteristics calculated from the physics-based simulation.

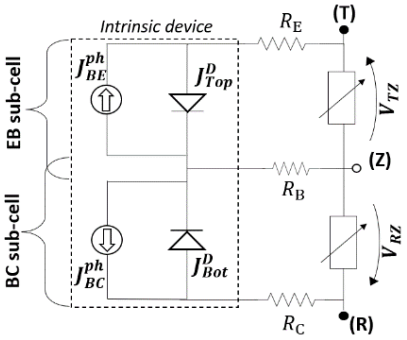

Figure 3: Equivalent circuit of the 3T-HBT tandem. Emitter, base and collector contacts are named as T, Z and R respectively, following the notation in [16].

The lumped parasitic resistances R_E R_B and R_C are estimated by analytical models of the grid unit cell [17], including lateral thin film and finger conduction, and contact resistance. In particular, with reference to the device structure in Fig. 1, the sheet resistance modeling the lateral transport across emitter and base is calculated as the parallel connection of the sheet resistances of their constituting thin film layers, e.g. ETL/n-Si for the base region of the HBT in Fig.1(a). The circuit simulation also accounts for the shadow loss due to the front metal grids. More details of the model will be discussed in the full work [18]. As seen in the equivalent circuit in Fig. 3, the impact of the base parasitic resistance, R_B, on the tandem performance is going to be more critical than the one of the emitter and collector resistances, because of the higher current flow across R_B.

3 RESULTS

To analyze the strength of the sub-cells cross-talk induced by the common base resistance, we start by considering a small-area device, with finger spacing and length of 1.5 mm and 1.5 cm, respectively.

Fig. 4 shows the interdependence of the MPP voltages of the two sub-cells and the corresponding efficiency reduction for several values of base sheet resistance, R_{sh}^{Base}.

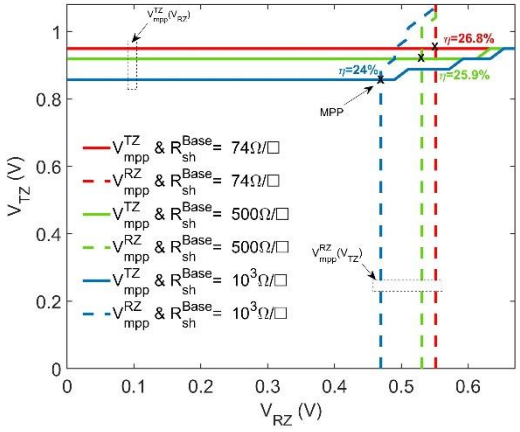

Figure 4: EB and BC MPP voltages ($V_{\mathrm{mpp}}^{\mathrm{TZ}}$ *and* $V_{\mathrm{mpp}}^{\mathrm{RZ}}$) as a function of V^{RZ} and V^{TZ} voltages.

For the tandem PVK/Si-homojunction tandem of Fig. 1(a), we estimated a base sheet resistance of ≈ 74 Ω/□, limited by the lateral transport across the (n^+)c-Si layer. Higher values might be representative of other tandem architectures on heterojunction Si cells, due to the high sheet resistance of the thin a-Si:H layers (up to 10^5 Ω/□). One can observe that the two sub-cells remain independent up to the MPP, regardless of the value of R_B. The R_B mediated cross-talk onsets only at voltages higher than the MPP one and causes an increase of the open circuit (OC) voltage as the bias of the other sub-cell grows towards OC, as observed experimentally in III-V HBT tandems [19]. Therefore, the R_B mediated interdependence between the sub-cells has a marginal impact on the attainable efficiency. On the other hand, for each sub-cell, V_{mpp} becomes smaller as R_B increases, because of the series resistance effect. In this sense, it is important to assess the implications in terms of scalability of the technology.

The efficiency reduction due to shadow and resistive losses caused by the metal grids is studied in Fig. 5 and Fig. 6. In Fig. 5, we analyze the impact of R_{sh}^{Base} in terms of efficiency loss for finger distance in the range [0.5 ÷10] mm, with finger length of 1.5 cm. We find that for a R_{sh}^{Base} up to 100 Ω/□, the efficiency loss can be minimized to less than 3% with finger distance in the range [1.5 ÷ 2.9] mm, in line with typical finger distance found in Si cells. Instead, by considering higher values of R_{sh}^{Base} ≈ 1000 Ω/□ (representative of PVS tandems on heterojunction c-Si cells), the finger spacing shall be reduced to about 1 mm, with a minimum efficiency penalty of ≈ 5%. Lower finger distance implies a higher penalty due to the dominant effect of shadow losses.

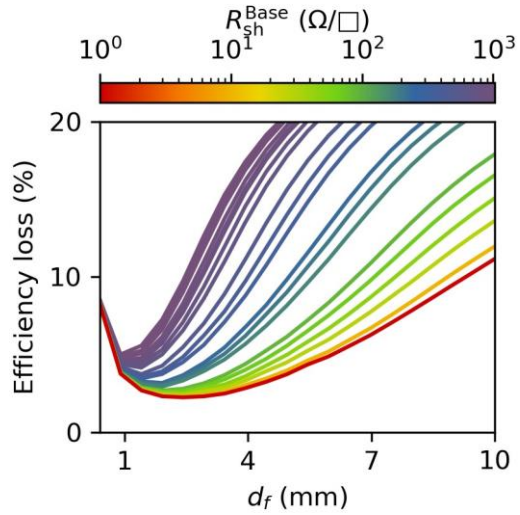

Figure 5: Efficiency loss as a function of the finger distance (d_f) and base sheet resistance (R_{sh}^{Base}).

Fig. 6 shows how the efficiency penalty scales with finger length and spacing, for an HBT with homojunction Si cell. With an optimized layout, efficiency loss remains lower than 5% for finger lengths up to about 8 cm, which is promising in the perspective of scaling up to large areas. The HBT with heterojunction Si cell is more critical, because of the low conductivity of the amorphous silicon layers, but still manageable by suitable design layouts, as discussed in the full paper [18].

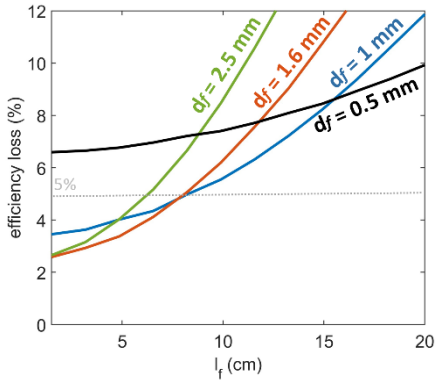

Figure 6: Efficiency loss as a function of finger length (l_f) and spacing (d_f) for a perovskite/silicon 3T-HBT on homojunction Si cell ($R_{sh}^{Base} \approx 74\ \Omega/\square$).

4 ACKNOWLEDGEMENTS

The authors acknowledge Francesco di Giacomo, Centre for Hybrid and Organic Solar Energy (CHOSE), University of Rome Tor Vergata for useful discussions. This research was partly funded by the ECSEL Joint Undertaking (JU) under grant agreement No. 101007247. The JU receives support from the European Union's Horizon 2020 research and innovation programme and Finland, Austria, Germany, Ireland, Iceland, Italy, Sweden, and Switzerland.

5 REFERENCES

[1] International technology roadmap for photovoltaic (ITRPV), 14th edition, (2023)

[2] Reddy, S. H., Di Giacomo, F., & Di Carlo, A. (2022). Low-temperature-processed stable perovskite solar cells and modules: a comprehensive review. Advanced Energy Materials, 12(13), 2103534.

[3] Gota, F., Langenhorst, M., Schmager, R., Lehr, J., & Paetzold, U. W. (2020). Energy yield advantages of three-terminal perovskite-silicon tandem photovoltaics. Joule, 4(11), 2387-2403.

[4] Warren, E. L., Deceglie, M. G., Rienäcker, M., Peibst, R., Tamboli, A. C., & Stradins, P. (2018). Maximizing tandem solar cell power extraction using a three-terminal design. Sustainable Energy & Fuels, 2(6), 1141-1147.

[5] Wagner, P., Tockhorn, P., Hall, S., Albrecht, S., & Korte, L. (2023). Performance of Monolithic Two-and Three-Terminal Perovskite/Silicon Tandem Solar Cells Under Varying Illumination Conditions. Solar RRL, 7(5), 2200954.

[6] Kanda, H., Dan Mihailetchi, V., Gueunier-Farret, M. E., Kleider, J. P., Djebbour, Z., Alvarez, J., ... & Connolly, J. P. (2022). Three-terminal perovskite/integrated back contact silicon tandem solar cells under low light intensity conditions. Interdisciplinary Materials, 1(1), 148-156.

[7] Messmer, C., Goraya, B. S., Nold, S., Schulze, P. S., Sittinger, V., Schön, J., ... & Hermle, M. (2021). The race for the best silicon bottom cell: Efficiency and cost evaluation of perovskite–silicon tandem solar cells. Progress in Photovoltaics: Research and Applications, 29(7), 744-759.

[8] Messmer, C., Schön, J., Lohmüller, S., Greulich, J., Luderer, C., Goldschmidt, J. C., ... & Hermle, M. (2022). How to make PERC suitable for perovskite–silicon

tandem solar cells: A simulation study. Progress in Photovoltaics: Research and Applications, 30(8), 1023-1037.
[9] Ballif, C., Haug, F. J., Boccard, M., Verlinden, P. J., & Hahn, G. (2022). Status and perspectives of crystalline silicon photovoltaics in research and industry. Nature Reviews Materials, 7(8), 597-616.
[10] International technology roadmap for photovoltaic (itrpv), 13th edition, april (2022)
[11] Park, I. J., Park, J. H., Ji, S. G., Park, M. A., Jang, J. H., & Kim, J. Y. (2019). A three-terminal monolithic perovskite/Si tandem solar cell characterization platform. Joule, 3(3), 807-818.
[12] Martí, A., & Luque, A. (2015). Three-terminal heterojunction bipolar transistor solar cell for high-efficiency photovoltaic conversion. Nature communications, 6(1), 6902.
[13] Antolín, E., Zehender, M. H., Svatek, S. A., Steiner, M. A., Martínez, M., García, I., ... & Martí, A. (2022). Progress in three-terminal heterojunction bipolar transistor solar cells. Progress in Photovoltaics: Research and Applications, 30(8), 843-850.
[14] Giliberti, G., Di Giacomo, F., & Cappelluti, F. (2022). Three Terminal Perovskite/Silicon Solar Cell with Bipolar Transistor Architecture. Energies, 15(21), 8146.
[15] Giliberti, G., & Cappelluti, F. (2022, March). Physical simulation of perovskite/silicon three-terminal tandems based on bipolar transistor structure. In Physics, Simulation, and Photonic Engineering of Photovoltaic Devices XI (Vol. 11996, p. 1199602). SPIE.
[16] Warren, E. L., McMahon, W. E., Rienacker, M., VanSant, K. T., Whitehead, R. C., Peibst, R., & Tamboli, A. C. (2020). A taxonomy for three-terminal tandem solar cells. ACS Energy Letters, 5(4), 1233-1242.
[17] Mette, A. (2007). New concepts for front side metallization of industrial silicon solar cells (Doctoral dissertation, Freiburg (Breisgau), Univ., Diss., 2007).
[18] Giliberti G, Cagnoni M. and Cappelluti F. (2023). Monolithic 3-terminal perovskite/silicon HBT-based tandem compatible with both-side contact silicon cells: a theoretical study. EPJ Photovoltaic. Accepted for publication. 10.1051/epjpv/2023024.
[19] Zehender, M. H. (2022). Three-terminal heterojunction bipolar transistor solar cells= Células solares de tres terminales tipo transistor bipolar de heterounión (Doctoral dissertation, Telecomunicacion).